

# DroPS

Deriving  $r$  from Power Spectra

Zhiqi Huang

[huangzhq25@mail.sysu.edu.cn](mailto:huangzhq25@mail.sysu.edu.cn)

October 28, 2025

# Contents

|          |   |           |
|----------|---|-----------|
| <b>1</b> | <b>Introduction</b>   | <b>3</b>  |
| 1.1      | Primordial power spectra . . . . .                                    | 3         |
| 1.2      | CMB B-polarization and $r$ . . . . .                                  | 3         |
| 1.3      | Ground-based CMB experiments with small-aperture telescopes . . . . . | 4         |
| <b>2</b> | <b>Software Documentation</b>   | <b>4</b>  |
| 2.1      | Installing DroPS . . . . .  | 4         |
| 2.1.1    | Installing Tools and Libraries . . . . .                              | 4         |
| 2.1.2    | Set up a python virtual environment . . . . .                         | 5         |
| 2.1.3    | Install requirements . . . . .  | 6         |
| 2.1.4    | Hack pysm3 . . . . .  | 7         |
| 2.2      | Base simulations . . . . .  | 7         |
| 2.2.1    | Generate a TOD filtering model . . . . .                              | 7         |
| 2.2.2    | Base simulations . . . . .  | 8         |
| 2.3      | Analyzing the sky maps . . . . .                                      | 8         |
| 2.3.1    | Analyzing one realization of sky . . . . .                            | 9         |
| 2.3.2    | Analyzing multiple realizations of sky . . . . .                      | 9         |
| 2.3.3    | How to apply on real data . . . . .                                   | 10        |
| 2.3.4    | Comparing with other pipelines . . . . .                              | 10        |
| 2.4      | Map-level Operations . . . . .  | 11        |
| 2.4.1    | Likelihood-based component separation . . . . .                       | 11        |
| <b>3</b> | <b>Technical Details</b>  | <b>11</b> |
| 3.1      | Foreground model . . . . .  | 11        |
| 3.2      | TOD filtering . . . . .   | 13        |
| 3.3      | Likelihood for band powers . . . . .                                  | 13        |
| 3.4      | Likelihood for map-level component separation . . . . .               | 13        |

# 1 Introduction

## 1.1 Primordial power spectra

According to the standard cosmological model, the cosmic microwave background (CMB) and the large-scale structure of the universe originated from tiny, nearly Gaussian metric fluctuations in the primordial universe. At linear order, these primordial metric fluctuations can be decomposed into scalar, vector, and tensor modes. Vector perturbations decay rapidly and are therefore generally assumed to be negligible. The primordial scalar and tensor perturbations are respectively parameterized by the dimensionless scalar power spectrum  $\mathcal{P}_S(k)$  and tensor power spectrum  $\mathcal{P}_T(k)$ , where  $k$  denotes the comoving wavenumber.

Guided by slow-roll inflation models, the primordial power spectra are commonly parameterized as

$$\mathcal{P}_S(k) = A_s \left( \frac{k}{k_{\text{pivot}}} \right)^{n_s-1}, \quad (1)$$

and

$$\mathcal{P}_T(k) = r A_s \left( \frac{k}{k_{\text{pivot}}} \right)^{n_t}. \quad (2)$$

The scalar amplitude  $A_s$  and spectral tilt  $n_s$  have been tightly constrained by CMB experiments [1]. In most viable inflationary scenarios, the tensor tilt  $n_t$  is very small; it is typically either fixed to zero or set to the slow-roll prediction  $n_t = -r/8$ . The tensor-to-scalar ratio  $r$  at the pivot scale, however, remains poorly measured. As of this writing, the best 95% confidence-level (CL) upper limit is  $r < 0.032$  [2]. Nevertheless, a broad range of inflationary models remains consistent with  $0 < r < 0.032$ .

## 1.2 CMB B-polarization and $r$

The search for the signature of primordial gravitational waves in CMB, i.e., measuring  $r$  from CMB is one of the most compelling pursuits in modern cosmology. This quest focuses on a unique observable: the B-mode polarization pattern.

The CMB photons became polarized when they scattered off free electrons in the early universe. This process imprinted a directional preference on the light, creating two distinct patterns: E-modes, which have a curl-free pattern like the electric field around charges, and B-modes, which have a curl-like pattern. While density fluctuations (scalar perturbations) in the primordial plasma can generate E-modes and a small amount of B-modes through gravitational lensing (so-called lensing B-modes), they cannot produce the specific, large-scale curl-like pattern of primordial B-modes.

This is where primordial gravitational waves come in. These waves, theorized to be generated during the inflationary epoch, are literally ripples in the fabric of spacetime.

As they propagated through the early universe, they periodically stretched and squeezed space, imparting a unique, curl-like distortion to the plasma. This gravitational tugging created a polarization pattern in the CMB that is fundamentally rotational in nature—the primordial B-mode polarization.

Therefore, the B-mode power spectrum at large angular scales acts as a direct tracer for these primordial gravitational waves. A confident detection of this primordial B-mode signal would be tantamount to detecting the gravitational waves themselves. Its amplitude is directly proportional to the energy scale of inflation, with the tensor-to-scalar ratio  $r$  quantifying the strength of the signal. Measuring this B-mode power spectrum thus provides a unique window into the physics of the universe’s first moments and the grand unification of gravity and quantum mechanics.

### 1.3 Ground-based CMB experiments with small-aperture telescopes

Many ground-based CMB experiments with small-aperture telescopes (SAT), such as BICEP/Keck [3], AliCPT [4], and Simons Observatory SAT (SO-SAT) [5] aim to measure the CMB B-mode polarization at degree scales and to constrain the primordial gravitational waves. These telescopes typically measure the sky emission in the range between 30GHz and 300GHz. The raw signals measured by these telescopes are mixture of Galactic foreground, CMB, shot noise, instrumental noise, and contamination from the ground and atmosphere. Extracting CMB B-mode polarization signal from the mixture of signals is a non-trivial problem and need to be dealt with by specialized softwares. DroPS is one of the software does this job, primarily designed for the ground-based small-aperture telescopes.

## 2 Software Documentation

### 2.1 Installing DroPS

The instruction here has been tested on Ubuntu-24.04.3LTS, and should be easily extendable to other linux platforms. A bit twists may need to be done if you are working with Windows or Mac-OS.

#### 2.1.1 Installing Tools and Libraries

Install the following packages and libraries with Synaptic Package Manager (or “sudo apt install”):

- git
- gcc
- gfortran
- cmake
- python3-pip
- python-is-python3
- python3-venv
- openmpi-dev
- libxcb-cursor0
- libcfitsio-dev
- libgsl-dev
- libfftw3-dev
- libfftw3-mpi-dev
- libhealpix-dev

### 2.1.2 Set up a python virtual environment

Create a directory for python virtual environment in your work path (hereafter denoted as YourWorkPath)

```
mkdir YourWorkPath/.work
```

Create the python virtual environment

```
python -m venv YourWorkPath/.work
```

Activate the virtual environment

```
source YourWorkPath/.work/bin/activate
```

On windows you may need to run

```
YourWorkPath/.work/Scripts/activate.bat
```

in cmd.exe or

```
YourWorkPath/.work/Scripts/activate.ps1
```

in PowerShell.

When you are done with your work, exit the terminal or use

```
deactivate
```

to exit the virtual environment.

If you are not working with other python projects. You may want to activate the virtual environment automatically with the terminal

```
echo "source YourWorkPath/.work/bin/activate" ~/.bashrc
```

### 2.1.3 Install requirements

Activate the virtual environment either manually or automatically as described in the previous subsection.

Upgrade pip for the latest information of packages:

```
pip install --upgrade pip
```

Now enter your work path where you want to install DroPS

```
cd YourWorkPath
```

Get the DroPS repository

```
git clone https://github.com/zqhuang/DroPS
```

Now enter the DroPS directory

```
cd DroPS
```

Install all dependences

```
pip install -r requirements.txt
```

#### 2.1.4 Hack pysm3

Hacking a python package is probably against the basic idea of python, but we are doing it anyway to improve the efficiency of CMB simulations. If you only want to analyze maps, however, you can skip this “unpleasant” step.

Enter the DroPS directory

```
cd YourWorkPath/DroPS
```

Move the cmb.py file in the pysm3 package to somewhere else

```
mv PATH_TO_pysm3/models/cmb.py cmb_backup.py
```

and replace it with the cmb.py file that comes with DroPS

```
cp cmb.py PATH_TO_pysm3/models/
```

Here PATH\_TO\_pysm3 stands for the path where pysm3 was installed. On Ubuntu 24.04.3LTS, you may find PATH\_TO\_pysm3 to be

YourWorkPath/.work/lib/python3.12/site-packages/pysm3

If you are not using Ubuntu24.04.3LTS, the pysm3 path may be slightly different. You can find out the path by doing

```
sudo apt install plocate
```

and

```
locate pysm3
```

## 2.2 Base simulations

### 2.2.1 Generate a TOD filtering model

A critical step in processing data from ground-based CMB experiments is the removal of contaminating ground and atmospheric signals from the time-ordered data (TOD). To simulate this filtering, one needs specific information about the experiment’s site, which is not currently available. Fortunately, the overall effect of the filtering is understood: it

suppresses large-scale (low multipole) power in the resulting maps and introduces non-Gaussianity by mixing different Fourier modes.

If you are not keen about simulating precise filtering effect for a specific experiment, you may use the “mock filtering” tool that comes with DroPS to generate a filtering matrix:

```
python mock_filtering.py
```

Follow the prompt and enter the healpix resolution (nside, 128 for testing, 256/512 for serious simulations) and the file name for the filtering matrix (e.g. filter\_128.pickle).

### 2.2.2 Base simulations

In this section, we run “base simulations” to obtain the statistics of the sky.

To begin with, you can simulate noise/cmb/foreground maps with a 4-channel ground-based experiment

```
python simulate.py Test/test_sim_config.txt
```

Read the configuration file Test/test\_sim\_config.txt to understand how the experiment is specified.

In this step, you generate a lot of noise and CMB maps based on the noise model and cosmology that are specified in the configuration file.

You also generate a foreground map in this step, based on the model ['d0', 's0'] that is specified in the configuration file. We are not able to generate “a lot of foreground maps”, as we do not really understand the details of the statistics of the Galactic emission. This ['d0', 's0'] foreground map only captures the gross feature of the Galactic emission. The “actual foreground” that we will analyze in the next section can be different from the one in the base simulations.

To understand what ['d0', 's0'] means. Follow the pysm3 documentation at <https://pysm3.readthedocs.io/>.

## 2.3 Analyzing the sky maps

In the last section, we run “base simulations” based on the known noise model, assumed foreground model (['d0', 's0']) and some assumed  $r$  values. In this section, we simulate the “observed sky” with the same noise model, optionally a different foreground model, and a  $r$  value that has nothing to do with the base simulations. DroPS will reconstruct  $r$  by comparing the “observed sky” with the base simulations.



### 2.3.1 Analyzing one realization of sky

Generate the “observed sky” with, e.g.,

```
python simulate.py Test/test_sim_config.txt maps/test_ 0.01 999
```

You can replace `maps/test_` with your preferred prefix for the output maps, `0.01` with your preferred fiducial  $r$  value, and `999` with your preferred random seed. To test whether DroPS can deal with a spatial variation of the foreground, you may also replace the `['d0', 's0']` foreground model with `['d1', 's1']` in the configuration file `Test/test_sim_config.txt`.

Now analyze the “observed sky” with

```
python mainpipe.py Test/test_ana_config.txt maps/test_
```

Read the configuration file `Test/test_ana_config.txt` to understand how to analyze the maps with different settings.

### 2.3.2 Analyzing multiple realizations of sky

In this step we will simulate the sky with many different random seeds, and analyze all the realizations of sky. The purpose is to test whether the measured  $r$  is biased or not.

This time we choose a different foreground model `["d1", "s1"]` (modify the configuration file `Test/test_sim_config.txt`, if you have not done so). Now run the simulations and analyze them by running the following shell script

Listing 1: Testing  $r$  bias

```
#!/bin/bash
for i in `seq 20`
do
    python simulate.py Test/test_sim_config.txt maps/test${i}_
0.01 ${i} d1s1
    python mainpipe.py Test/test_ana_config.txt maps/test${i}_
Test/r1_logfile_d1s1.txt
done
```

Plot the result

```
python utils/plot_rs.py Test/r1_logfile_d1s1.txt 0.01
```

Here `0.01` is the fiducial value of  $r$  used in simulations (see the content of `test_bias.sh`), used to plot the solid orange line. The mean of reconstructed mean values of  $r$  (dotted

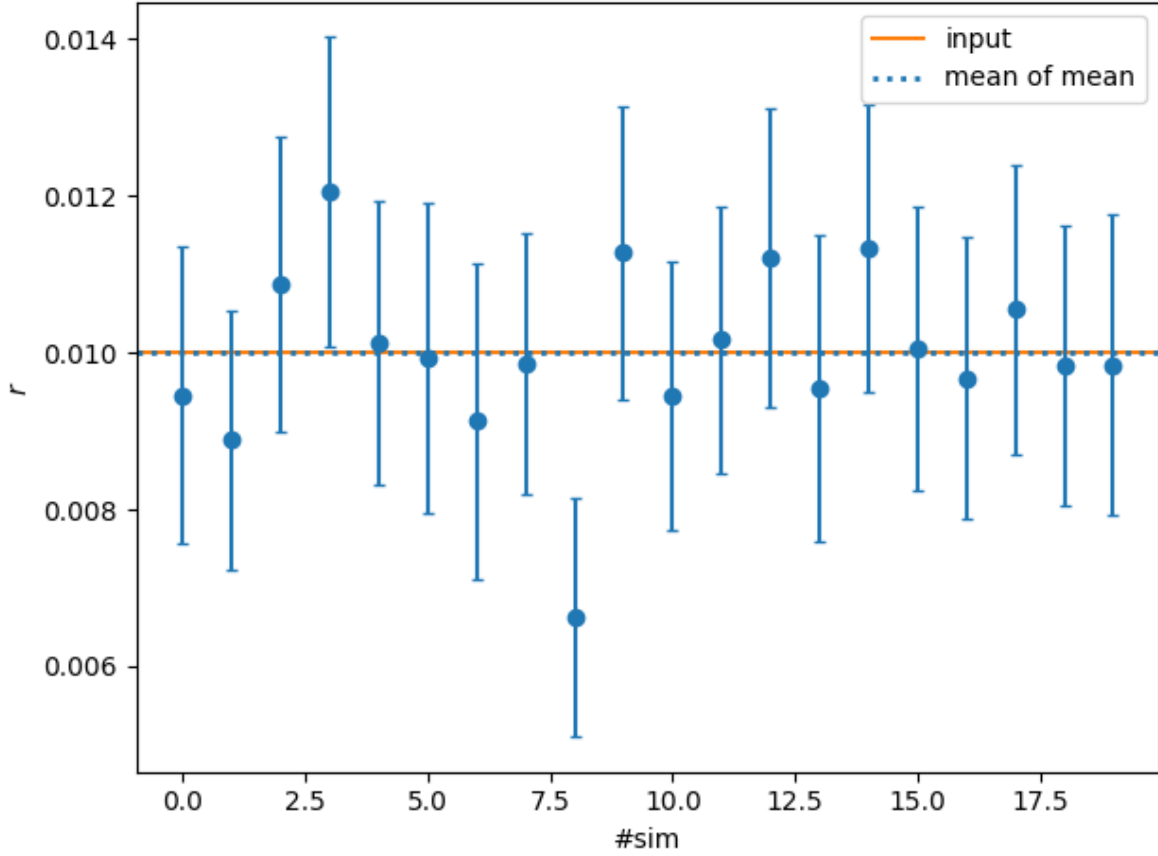


Figure 1: Reconstructed  $r$  for 20 skys with different random seeds. For each sky, the  $r$  value is reconstructed by comparing the sky with 300 simulations. The 20 skys are simulated with foreground model ['d1', 's1'] (spatially varying SED of synchrotron and dust emission), while ['d0', 's0'] (fixed SED) is used in the 300 simulations.

blue line) is supposed to be close to the fiducial value for an unbiased estimator, as shown in Figure 1.

### 2.3.3 How to apply on real data

A real experiment comes with its own pipeline of noise simulations and TOD filtering, and provides the actually observed sky maps. To analyze the real data, you can simply replace the base simulations with the maps from the simulation pipeline of the experiment, and replace the realization of sky with the actually observed ones.

### 2.3.4 Comparing with other pipelines

DroPS has been applied on AliCPT data challenge (simulated 14% sky, 95GHz and 150GHz) and achieved consistent results with other methods [6]. Here we further compare DroPS with three pipelines that have been applied on simulation data of SO-SAT (Wolz

et al. 2024 [5]). We adopt the optimistic configuration of SO-SAT. The input fiducial  $r$  is zero, and in the analyses nonphysical negative  $r$  is allowed<sup>1</sup>. The results are shown in Figure 2. From top to bottom, foreground models [“d0”, “s0”], [“d1”, “s1”], and [“dm”, “sm”] are used, respectively. From the left where the reconstructed mean values of  $r$  and the bias (mean of the mean values of  $r$ ) are shown, we find DroPS has negligible biases for all cases and more stable than the three pipelines tested in Wolz et al. The right column shows  $\sigma_r$ , the statistical uncertainties in  $r$ . We again find good consistency between DroPS and the other pipelines.

## 2.4 Map-level Operations

### 2.4.1 Likelihood-based component separation

The most well known method of component separation is probably the internal linear combination (ILC) algorithm and its variations. The basic idea is to isolate a signal - whose frequency dependence is known - by taking linear combination of the frequency maps. To do that in pixel space, the frequency maps have to be smoothed to a common resolution.

For ground-based CMB experiments, however, a key challenge of ILC or ILC-like methods is that TOD filtering and beam convolution are non commutative operations. This prevents the frequency maps from being smoothed to a common resolution. Thus, while ILC remains popular in studies where the complexity of TOD filtering effect is ignored [5], likelihood-based method - which requires much more computing resources - has been used in real data analyses of BICEP/Keck [7].

## 3 Technical Details

### 3.1 Foreground model

The frequency dependence of dust temperature fluctuation is

$$W_d(\nu) = \left( \frac{\nu}{\nu_{\text{ref}}} \right)^{\beta_d - 1} e^{\frac{h(\nu_{\text{ref}} - \nu)}{k_B T_{\text{CMB}}}} \left( \frac{e^{\frac{h\nu}{k_B T_{\text{CMB}}}} - 1}{e^{\frac{h\nu_{\text{ref}}}{k_B T_{\text{CMB}}}} - 1} \right)^2 \left( \frac{e^{\frac{h\nu_{\text{ref}}}{k_B T_{\text{MBB}}}} - 1}{e^{\frac{h\nu}{k_B T_{\text{MBB}}}} - 1} \right). \quad (3)$$

The frequency dependence of synchrotron temperature fluctuation is

$$W_s(\nu) = \left( \frac{\nu}{\nu_{\text{ref}}} \right)^{\beta_s - 2} e^{\frac{h(\nu_{\text{ref}} - \nu)}{k_B T_{\text{CMB}}}} \left( \frac{e^{\frac{h\nu}{k_B T_{\text{CMB}}}} - 1}{e^{\frac{h\nu_{\text{ref}}}{k_B T_{\text{CMB}}}} - 1} \right)^2. \quad (4)$$

---

<sup>1</sup>in DroPS this is realized by setting `r_lowerbound` negative in the configuration file

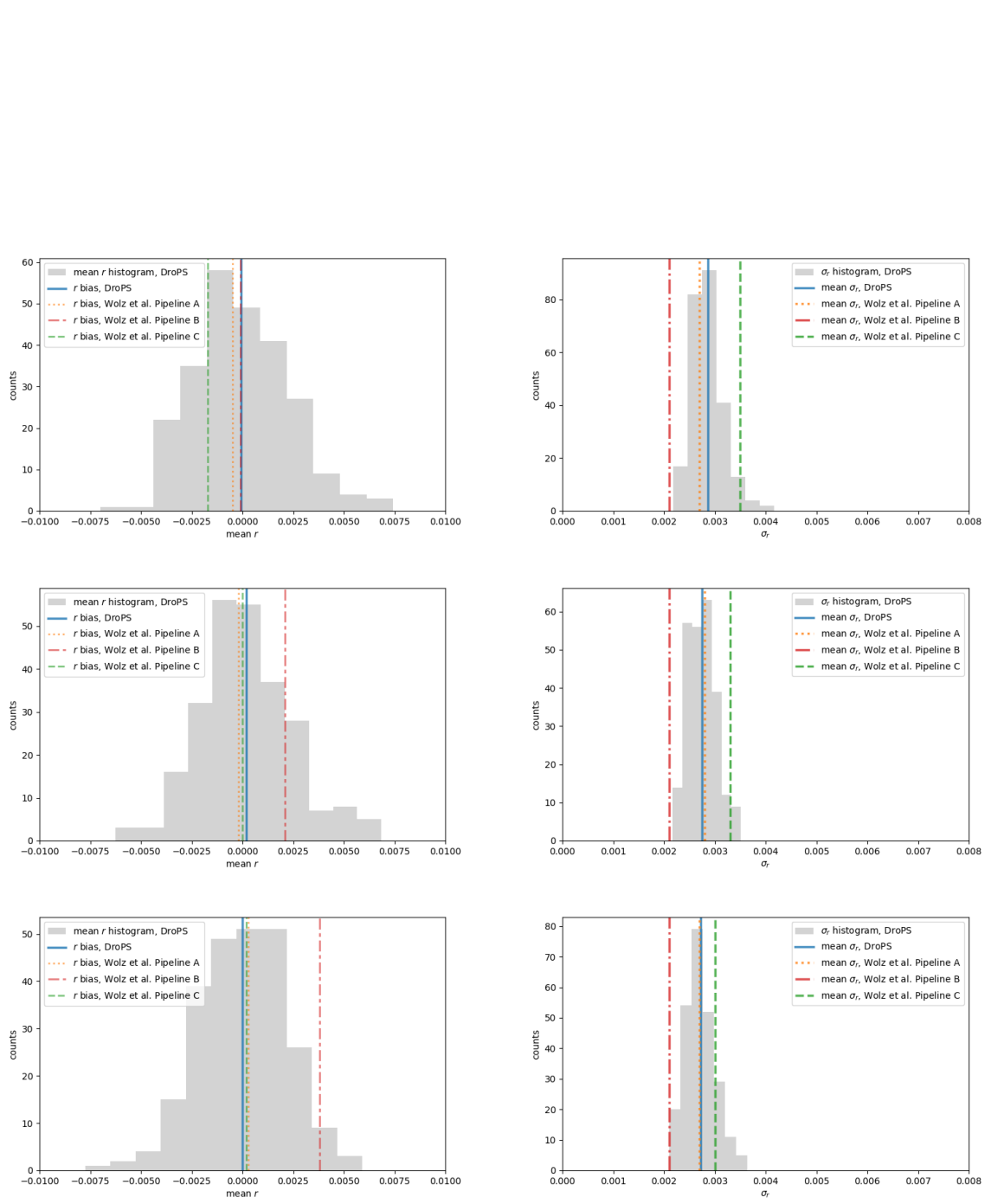


Figure 2: Comparing DroPS with three pipelines that are described in Wolf et al. [5]. From top to bottom, foreground models “d0, s0”, “d1, s1”, and “dm, sm” are used, respectively. Left and right columns are the distribution of reconstructed mean  $r$  and  $\sigma_r$ , respectively.

### 3.2 TOD filtering

### 3.3 Likelihood for band powers

### 3.4 Likelihood for map-level component separation

The likelihood  $\mathcal{L} \propto e^{-\chi^2/2}$  is based on a Gaussian noise model

$$\chi^2 = v_{\text{noise}}^T N^{-1} v_{\text{noise}}, \quad (5)$$

where  $v_{\text{noise}}$  is the noise frequency maps inferred from a sky model and the observed frequency maps, and  $N$  is the covariance of  $v_{\text{noise}}$ . In pixel space, the size of each vector is  $n_{\text{pix}}n_f$ , i.e., product of the number of pixels and the number of frequency channels. For AliCPT or SO-SAT and maps with degree-scale resolution, we typically have  $n_{\text{pixel}}n_{\text{frequency}} \gtrsim 10^4$ . The number of elements in the covariance matrix  $N$  is  $\gtrsim 10^8$ , which is difficult to estimate with simulations and also difficult to invert. The BICEP/Keck analysis [7] only considers pixel auto-correlation, that is, the diagonal approximation of  $N$  in pixel space. A better approximation, which will be used in DroPS, is a diagonal form of  $N$  in harmonic space.

We label a pixel with index  $j$  ( $j = 1, 2, \dots, n_{\text{pix}}$ ), and frequency channels with index  $k$  ( $k = 1, 2, \dots, n_f$ ). The CMB maps are identical in all frequency channels, and are modeled as

$$(Q \pm iU)_{\text{CMB},j,k} = - \sum_{\ell=0}^{\ell_{\text{max}}} \sum_{m=-\ell}^{\ell} (c_{\ell m}^E \pm i c_{\ell m}^B) {}_{\pm 2}Y_{\ell m}(\mathbf{n}_j), \quad (6)$$

where  $\mathbf{n}_j$  is the directional vector of the  $j$ -th pixel. Note that here  $c_{\ell m}^E$  and  $c_{\ell m}^B$  are harmonic coefficients of the full-sky CMB map. Degeneracy between these parameters are expected for partial sky observations.

Due to limited frequency resolution, BICEP/Keck model  $v_{\text{FG}}$  as a single component (thermal dust). DroPS takes a more accurate two-component model with emission from Galactic synchrotron and thermal dust. The dust maps are modeled as

$$(Q \pm iU)_{\text{dust},j,k} = - \int W_d(\nu) f_k(\nu) d\nu \sum_{\ell=0}^{\ell_{\text{max}}} \sum_{m=-\ell}^{\ell} (d_{\ell m}^E \pm i d_{\ell m}^B) {}_{\pm 2}Y_{\ell m}(\mathbf{n}_j), \quad (7)$$

where the frequency dependence function  $W_d$  is defined in Eq. (3) and  $f_k(\nu)$  is the frequency distribution of the  $k$ -th frequency channel. Synchrotron maps are modeled similarly,

$$(Q \pm iU)_{\text{sync},j,k} = - \int W_s(\nu) f_k(\nu) d\nu \sum_{\ell=0}^{\ell_{\text{max}}} \sum_{m=-\ell}^{\ell} (s_{\ell m}^E \pm i s_{\ell m}^B) {}_{\pm 2}Y_{\ell m}(\mathbf{n}_j), \quad (8)$$

where  $W_s$  is given in Eq. (4).

The sky model  $(Q + iU)_{\text{sky}}$  is the sum of Eqs. (6, 7, 8). Passing the sky model through the TOD filtering and map making process, we obtain the filtered sky maps. Subtracting the filtered sky maps from the observed (filtered) maps, we obtain filtered noise maps in pixel space. To compute the likelihood, we decompose the noise maps into harmonic space,

$$M_j(Q \pm iU)_{\text{noise,filtered},j,k} = - \sum_{\ell=0}^{\ell_{\max}} \sum_{m=-\ell}^{\ell} (\tilde{n}_{\ell m}^E \pm i\tilde{n}_{\ell m}^B) {}_{\pm 2}Y_{\ell m}(\mathbf{n}_j). \quad (9)$$

Here  $M_j$  is pixel value of a smoothed mask (default: apodization with 2 degrees and “C2”). The purpose of introducing such a smoothed mask is to avoid large edge effect on the estimation of pseudo harmonic coefficients  $\tilde{n}_{\ell m}^E$  and  $\tilde{n}_{\ell m}^B$ .

On the other hand, we can calculate  $\tilde{n}_{\ell m}^E$  and  $\tilde{n}_{\ell m}^B$  from the filtered noise maps in the base simulations, and compute their diagonal covariance  $\tilde{N}_{\ell m}^E \equiv \langle |\tilde{n}_{\ell m}^E|^2 \rangle$  and  $\tilde{N}_{\ell m}^B \equiv \langle |\tilde{n}_{\ell m}^B|^2 \rangle$ .

## References

- [1] Nabila Aghanim, Yashar Akrami, Mark Ashdown, et al. Planck 2018 results-vi. cosmological parameters. *Astronomy & Astrophysics*, 641:A6, September 2020.
- [2] M. Tristram, A. J. Banday, K. M. Górski, R. Keskitalo, C. R. Lawrence, K. J. Andersen, R. B. Barreiro, J. Borrill, L. P. L. Colombo, H. K. Eriksen, R. Fernandez-Cobos, T. S. Kisner, E. Martínez-González, B. Partridge, D. Scott, T. L. Svalheim, and I. K. Wehus. Improved limits on the tensor-to-scalar ratio using BICEP and Planck data. *Physical Review D*, 105(8):083524, April 2022.
- [3] P. A. R. Ade, Z. Ahmed, M. Amiri, et al. BICEP/Keck XV: The BICEP3 Cosmic Microwave Background Polarimeter and the First Three-year Data Set. *Astrophysical Journal*, 927(1):77, March 2022.
- [4] Hong Li, Si-Yu Li, Yang Liu, Yong-Ping Li, and Xinmin Zhang. Tibet’s window on primordial gravitational waves. *Nature Astronomy*, 2:104–106, February 2018.
- [5] Kevin Wolz, Susanna Azzoni, Carlos Hervías-Caimapo, Josquin Errard, Nicoletta Krachmalnicoff, David Alonso, Carlo Baccigalupi, Antón Baleato Lizancos, Michael L. Brown, Erminia Calabrese, Jens Chluba, Jo Dunkley, Giulio Fabbian, Nicholas Galitzki, Baptiste Jost, Magdy Morshed, and Federico Nati. The Simons Observatory: Pipeline comparison and validation for large-scale B-modes. *Astronomy & Astrophysics*, 686:A16, June 2024.

- [6] Junzhou Zhang, Shamik Ghosh, Jiazheng Dou, Yang Liu, Siyu Li, Jiming Chen, Jiaxin Wang, Zhaoxuan Zhang, Jacques Delabrouille, Mathieu Remazeilles, Chang Feng, Bin Hu, Hao Liu, Larissa Santos, Pengjie Zhang, Wen Zhao, Le Zhang, Zhi-Qi Huang, Hong Li, and Xinmin Zhang. Forecast of Foreground Cleaning Strategies for AliCPT-1. *Astrophysical Journal Supplement Series*, 274(2):26, October 2024.
- [7] BICEP/Keck Collaboration, P. A. R. Ade, Z. Ahmed, M. Amiri, D. Barkats, R. Basu Thakur, et al. BICEP/Keck XX: Component-separated maps of polarized CMB and thermal dust emission using Planck and BICEP/Keck Observations through the 2018 Observing Season. *arXiv e-prints*, page arXiv:2509.21648, September 2025.